Nuclear Inst. and Methods in Physics Research, A 941 (2019) 162350

Contents lists available at ScienceDirect

Nuclear Inst. and Methods in Physics Research, A

journal homepage: www.elsevier.com/locate/nima

Electrodeposition of low-enriched uranium onto small platinum electrodes

Michael A. Reichenberger [a,*], Daniel M. Nichols [a], Kevin Tsai [b], Sarah R. Stevenson [a], Tanner M. Swope [a], Caden W. Hilger [a], Joseph D. Hewitt [a], Katharine E. Kellogg [a], Jeremy A. Roberts [a], Cheng-Hung Chen [c], Douglas S. McGregor [a]

[a] S.M.A.R.T. Laboratory, Mechanical and Nuclear Engineering Department, Kansas State University, Manhattan, KS 66506, USA
[b] Idaho National Laboratory, Idaho Falls, ID 83402, USA
[c] Synova U.S.A, Secaucus, NJ 07094, USA

ARTICLE INFO

Keywords:
Neutron detector
In-Pile instrumentation
Electrodeposition
Fission chamber
Micro-Pocket Fission Detector
MPFD

ABSTRACT

An updated method of preparing thin, uranium-coated, 0.25-mm diameter platinum electrodes using the cyclic potential sweep method is described. Sixty-four samples were prepared using a 0.2 M $UO_2(NO_3)_2$ solution with 19.695% enriched uranium. Improvements were made to the sample preparation, electrodeposition, and analysis methods, producing smoother samples with more uniform surface features than prior work. Alpha-particle spectrometry was used to determine the mass of uranium deposited on each sample. The average mass of uranium deposited on the metallic electrode from 100 potential sweep cycles was 0.987×10^{-7} g with a standard deviation of 0.860×10^{-7} g. Removing the outliers reduces the average deposited mass to 0.741×10^{-7} g with a standard deviation of 0.410×10^{-7} g. A smooth, uniform deposition was observed over the entire electrode after deposition and no cracking or crystalline formations were observed. This improved method of electrodeposition remains an attractive method of depositing fissile material onto small metallic substrates for the fabrication of Micro-Pocket Fission Detectors.

1. Introduction

The continued development of Micro-Pocket Fission Detectors (MPFDs) requires the accurate deposition and characterization of fissile material onto metallic substrates [1–5]. MPFDs, which are constructed with radiation and temperature resistant materials, are designed to provide a real-time neutron flux measurement in high-flux environments without significantly perturbing the local neutron flux [5]. A thin fissile layer situated between parallel anode and cathode wires converts incident neutrons into energetic fission fragments. The fission fragments ionize gas within the detector chamber as illustrated in Fig. 1. An applied bias between the parallel anode and cathode wires causes charge motion within the chamber which is measured by a charge-sensitive pre-amplifier. Typical MPFDs utilize uranium as a neutron conversion material. A very thin deposition of neutron sensitive material (<1.0 μg) is required to achieve a sensitivity on the order of 10^{-9} interactions per unit flux [6].

Alpha particle sources and ion-beam targets are commonly fabricated by electrodeposition of actinide layers [7–9]. Preparation of targets using organic solutions (isopropyl alcohol, acetone, and ethanol) commonly offer uniform layer thicknesses but have been observed to suffer from poor reproducibility [10]. Previous research developed a method by which thin layers of uranium and thorium were deposited onto circular platinum electrodes using a cyclic potential sweep method [11]. Fissile material was deposited onto electron-beam evaporated metallic electrodes ranging from 0.3-mm to 2-mm in diameter located on either silicon dioxide or alumina substrates. Inconsistencies were observed upon the electrodeposited substrate including crystalline formations and regions void of electrodeposited material [11]. These inconsistencies were attributed to deficiencies in the electrode fabrication process and surface features of the insulating substrates.

The present work includes improvements to substrate fabrication methods, preparation methods for the electrolytic solution, and subsequent analysis of the electrodeposited samples. In contrast to prior work which used machined alumina substrates which suffered from poor surface roughness and electrode non-uniformities [11], sample substrates for the present work were fabricated using metal-liftoff techniques on a polished 99.6% alumina wafer. After contact evaporation and mask removal, sample discs were cut from the wafer using a Laser Micro-Jet® system [12]. The solution preparation method, based on prior work, continued to utilize the cyclic potential sweep method as a controlled means of electrochemically assisted deposition of uranium compared to the more commonly used potential-step method [11]. However, smaller solution batches were developed due to the low availability of fissile material. Low-Enriched Uranium (LEU) was used to demonstrate the effectiveness of the improved system. The increased activity of

* Corresponding author.
E-mail address: mar89@ksu.edu (M.A. Reichenberger).

https://doi.org/10.1016/j.nima.2019.162350
Received 10 April 2019; Received in revised form 10 June 2019; Accepted 3 July 2019
Available online 8 July 2019
0168-9002/

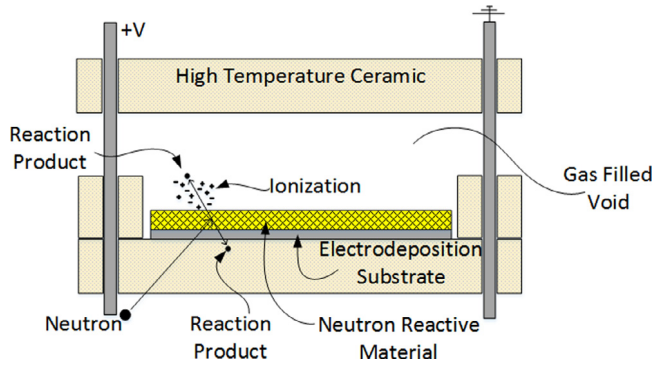

Fig. 1. Micro-Pocket Fission Detectors use an electrodeposited fissile layer to convert neutrons to fission fragments.

the 19.695% enriched LEU reduced the measurement time required to achieve 2% uncertainty in the alpha-particle activity measurement which was utilized to determine the mass of uranium deposited on the substrate surface. Finally, 64 samples were electrodeposited and analysed under the same experimental conditions to determine the relative consistency that was possible with the improved system.

2. Experimental methods

The production of sample discs for electrodeposition of LEU included three steps: electrode evaporation and disc fabrication, solution preparation, and electrodeposition.

2.1. Electrode fabrication

101.6-mm diameter, 0.5-mm thick, polished, 99.6% pure alumina wafers were electron-beam evaporated with 0.5-mm diameter circular metallic electrodes. A metal lift-off technique with a photomask was used to enhance electrode uniformity compared to physical shadow masked which were used in the past. The class-100 cleanroom facility at the Kansas State University S.M.A.R.T. Laboratory was utilized for wafer preparation, photolithography, metal evaporation, and metal lift-off procedures.

First, the wafer was rinsed and dried in the automatic spin-rinse dryer with de-ionize water for 3 cycles of 50/100/100 s respectively. The wafer was then dried at 250 °C for 20 min and allowed to cool for 5 min. Nitrogen was used to ensure no foreign material was left on the wafer before depositing 5 ml of AZ2070 negative photoresist on the centre of the wafer. The spinner was set to 1000 rpm for 5 s and then accelerated to 3000 rpm (at 1200 rpm/s) for 30 s. After allowing the wafer to stop spinning and to rest for 1 min, the wafer was baked on a 100 °C hot-plate for 3 min and allowed to cool for an additional 5 min. A pre-manufactured photomask was fabricated with the desired pattern to provide approximately 300 circular contacts spaced evenly on the wafer (the specific design was used to facilitate fabrication into MPFD components with 0.25-mm electrodeposition contacts). The wafer, with photoresist, was exposed to a 325 mJ/cm^2 intensity UV lamp for 15 s, allowed to sit for 5 min, then baked at 115 °C for an additional 1.5 min, and allowed to cool for five minutes, all in a dark environment. An MIF 300 developer bath was used to remove the undeveloped photoresist by dunking the wafer 60 times. The wafer was then rinsed in a de-ionized water cascade, rinsed in the spin-rinse dryer for 3 cycles of 50/100/100 s, and inspected with a microscope to ensure proper mask development, shown in Fig. 2.

In conformity with prior work [11], a layered Ti/Pt contact was evaporated to be used as the electrodeposition electrode. A 50 Å Ti layer was evaporated first onto the wafer with the photomask applied to aid in the adhesion of the following 500 Å Pt layer. Platinum was

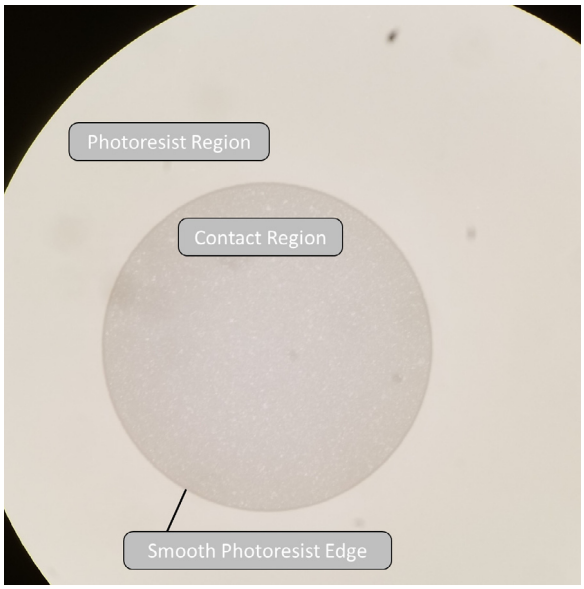

Fig. 2. The use of a photomask enhanced the uniformity and edge quality of the evaporated metallic electrodes which were used for electrodeposition.

Table 1
Optimized processing parameters for Micro-Jet® fabrication of MPFD discs were identified.

	Parameter	Setting
System	Machine type	LDS 200
	Helium flow (MFC)	0.9 NI/min
	Working distance	15 mm
	SHG temperature	30.0 °C
	Internal power	30 W
	Transmission	64.7%
Micro-Jet®	Nozzle diameter	50 μm
	Micro-Jet® diameter	42 μm
	Water pressure	300 bar
	Assist gas	Helium
Laser	Laser type	High power laser
	Wavelength	532 nm
	Pulse frequency	10 kHz
	Power in Jet	19.4 W
	Pulse width	180 ns

selected as the electrodeposition substrate for MPFDs because of its resistance to corrosion, low neutron-absorption cross-section, and high melting-point [11]. The wafer and electron-beam evaporation chamber were allowed to cool for 30 min before being removed. The metal lift-off procedure was performed by allowing the evaporated wafer to soak in a heated KWIK Strip® bath for 2 h, removing photoresist and excess metal around the desired features. The wafer was then sent out to have individual discs to be cut out using a Laser Micro-Jet® [12].

The Laser Micro-Jet® allowed for the fabrication of discs with five holes, necessary for eventual MPFD fabrication, to be cut with high-precision without affecting the metallic electrodes. The Laser Micro-Jet® combines conventional laser cutting techniques with a transparent water jet to precisely guide the laser bean using total internal reflection. The low-pressure water jet cools the cutting zone and removes debris, to facilitate accurate cutting of small features in materials which are typically difficult to machine, with a fine cut edge. Trials were performed with test wafers to identify the optimized parameters summarized in Table 1. Although the back-side of the alumina discs did appear rougher than the front side after the manufacturing process, the surface of the metallic electrodes remained smooth and uniform (shown in Fig. 3), an important improvement from prior work.

The completed MPFD discs were inspected using an Hitachi S-3400N scanning electron microscope. The holes and electrodes were

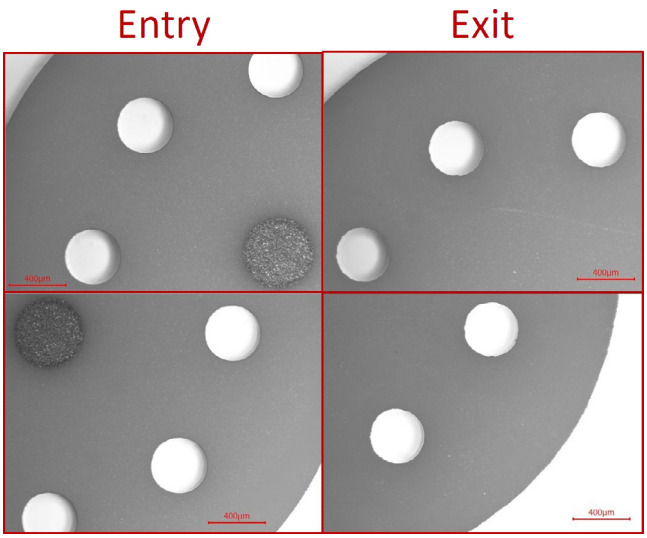

Fig. 3. MPFD discs were fabricated using a Laser Micro-Jet® without affecting the metallic electrodes. Two views of the entry (front) and exit (back) of an MPFD disc are shown.

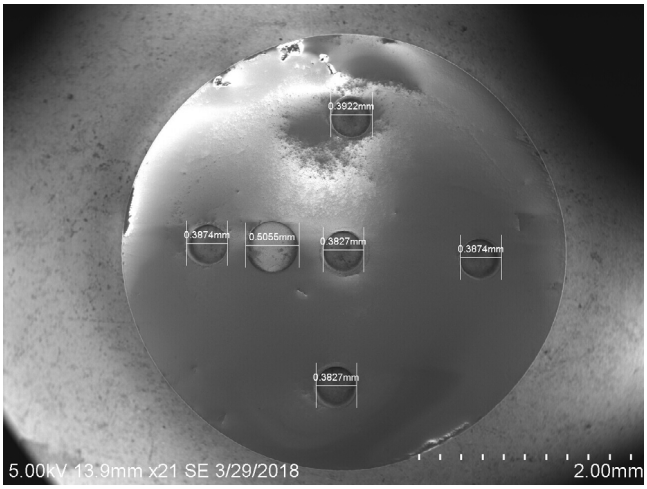

Fig. 4. The improved fabrication techniques yielded MPFD discs with more uniform features than prior work.

measured to ensure uniformity between samples as shown in Fig. 4. The surface roughness (S_a) of the completed discs was also measured to be S_a = 0.21 μm using a Keyence VK-X260K 3D Laser Scanning Confocal Microscope. As a point of reference, samples which were used for prior work were also analysed, yielding a surface roughness of S_a = 0.73 μm using the same system. Surface roughness was not previously measured [11].

2.2. Solution preparation

Anhydrous uranyl nitrate (>99%) with 19.695% enriched uranium was used as the source of fissile material for the 0.2 M $UO_2(NO_3)_2$ electrolytic solution. Prior to the solution preparation, necessary glassware was cleaned using a 4-step process (HNO_3, acetone, isopropyl alcohol, and deionized water) process. The HNO_3 was used to remove any residual fissile material from previous experiments, the acetone and isopropyl alcohol were used clean the surface, and the deionized water was used to rinse the glassware clean of any residual solvents. An Ohaus AR0650 scale was used to weight 1801.25 mg of ammonium nitrate and 51.25 mg of anhydrous uranyl nitrate which were combined in a 50-ml beaker. Deionized water was added to the beaker to bring the solution to approximately 10 ml. A syringe was used to measure 1.25 ml of 190 proof ethanol, which was then added to the electrolytic solution. The solution was finally topped off with deionized water to 18.75 ml. Prior work established a repeatable pH of 3.4 for uranium-based electrolytic solution using the aforementioned process with positive electrodeposition results [11]. The small solution volume prohibited the use of a pH meter to measure the solution pH. Therefore, litmus paper was used to confirm that the solution pH was between 3 and 4. Solution constituents are summarized in Table 2. The solution was used immediately for electrodeposition, and new solution was created for all subsequent electrodeposition trials using the same process.

Table 2
Composition of the 0.2 M uranium-containing electrolytic solution was based on the successful solution developed by previous work [11].

Component	0.2 M $UO_2(NO_3)_2$
19.695% Enriched uranyl nitrate	51.25 mg
Ammonium nitrate	1801.25 mg
190 Proof ethanol	1.25 ml

2.3. Cyclic voltammetry

The same electrodeposition cell and method were used for the LEU electrodeposition as were reported previously [11]. Each MPFD disc was rinsed with isopropyl alcohol and allowed to dry before being submerged in the electrolytic solution. A CH Instruments CHI600E electrochemical analyzer was used with three electrodes connected as illustrated in Fig. 5. The Ag/AgCl reference electrode was procured from CH Instruments, contained in a PTFE and glass vial with 3.0 M KCl reference solution. A 3-dimensional stage was positioned below the petri dish containing the electrolytic solution to allow for manual alignment of the working electrode probe with the working electrode. The working electrode probe and counter electrode were spaced approximately 1-cm apart from one another and were not moved between samples. A Leica DMS300 microscope was used to visually confirm contact between the electrode probe and the sample electrode (together making the counter electrode).

The electrodeposition parameters were determined previously [11]. The potential sweep range from −0.62 V to −0.64 V yielded consistent surface deposition using a 0.01 Vs^{-1} sweep rate. Each MPFD disc was electrodeposited using 100 potential sweep cycles, each cycle including two sweeps, one down −0.64 V and then back up to −0.62 V. Very little hydrogen evolution was observed (in the form of bubbling) during the electrodeposition process. Most samples produced no bubbles at all during the 100 cycles. Room temperature was not monitored, but no additional heating or cooling was utilized for the electrodeposition. Cyclic voltammograms were captured for each of the MPFD discs which were electrodeposited. A characteristic decrease in maximum current was observed on the cyclic voltammograms for each sample, with a representative plot shown in Fig. 6. After electrodeposition, each disc was rinsed with isopropyl alcohol and allowed to air-dry before being placed in individual containers.

3. Analysis of electrodeposited discs

The sample discs were inspected before and after electrodeposition using a scanning electron microscope to ensure that the surface was not damaged in the electrodeposition process. Visual inspection first confirmed the deposition of uranium onto each sample. The metallic working electrode changed from silver to golden in colour as uranium was deposited on the surfaces as shown in Fig. 7. Previously documented inconsistencies on the surface of electrodeposited discs were not observed on any of the discs comprising the present work. The electrode surface appeared to be uniformly coated for each disc, however

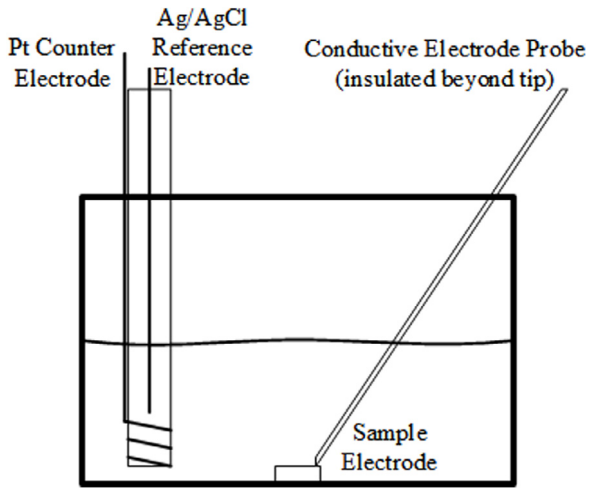

Fig. 5. A reference electrode, counter electrode, and working electrode were used to electrodeposit uranium from the electrolytic solution onto the metallic sample electrode, reproduced from [11].

regions on both sides of the circular electrode appeared have resisted electrodeposition, shown in Fig. 7. These regions were present on every sample, before and after electrodeposition, and it was determined that these regions were void of platinum, likely having been removed in the metal lift-off process. The sample activities were then measured using modular alpha-particle spectrometry chambers equipped with Ametek Ultra® ion-implanted alpha-particles detectors under a rough vacuum (maintaining 1000 mTorr pressure). The pulse-height spectrum acquired from each sample was analysed to determine the total alpha-particle activity of the sample, and subsequently the mass of the sample [11]. Only measured pulses occurring in the region of interest were attributed to decay from uranium, shown in Fig. 8. The specific activity of 19.695% enriched uranium was determined to be 3.63×10^5 Bq/g by linearly interpolating between published values for 20% and 10% enriched uranium [13].

The uranium masses for the samples, derived from the activity measurements, were used to determine the average and standard deviation of uranium deposited using the described method. The error of each measurement was determined from the number of counts which were observed in the region of interest, an example of which is shown in Fig. 8. Corrections were made for detector efficiency (ranging from 61% to 65% intrinsic efficiency), solid angle (approximately 40%), and background. Background measurements were conducted for all 16 alpha-particle spectrometry chambers in the weeks preceding the measurements, yielding background count rates between 3×10^{-5} and 8×10^{-3} cps. Mass error due to counting statistics alone therefore ranged from 0.84% to 4.75%, detailed in Table 3. The total mass of 19.695% enriched uranium deposited on each sample is shown in Fig. 9, with an average deposition of 0.987×10^{-7} g and with a standard deviation of 0.860×10^{-7} g. Removing the outliers reduces the average deposited mass to 0.741×10^{-7} g with a standard deviation of 0.410×10^{-7} g, shown in Fig. 9.

4. Conclusions

The electrodeposition of 19.695% LEU onto 0.25-mm platinum electrodes was tested using a previously developed cyclic-voltammetric procedure, utilizing a 0.2 M $UO_2(NO_3)_2$. Uranium mass deposited on the sample electrodes from 100 potential sweep cycles varied from 4.57×10^{-7} g ($\pm 0.0439 \times 10^{-7}$ g) to 0.120×10^{-7} g ($\pm 0.094 \times 10^{-7}$ g), with an average uranium mass of 0.987×10^{-7} g and with a standard deviation of 0.860×10^{-7} g. Removing the outliers reduces the average deposited mass to 0.741×10^{-7} g with a standard deviation of 0.410×10^{-7} g. The cyclic voltammograms conformed to prior research, and uranium was observed (both visually and by alpha-particle spectrometry) on the samples following electrodeposition. The physical characteristics (colour and surface features) appeared more consistent than with prior work. A smooth deposition was observed on all samples with no visible discrepancies on the surface, in contrast to prior work, where cracking, crystallization, and voids were observed. The quality and variation of the amount of uranium mass on the electrodeposited samples also conformed with prior research which suggested poor uniformity and high quality of electrodeposition using organic electrolytes [10]. Activity measurements of 7 samples yielded masses of more than twice the average value of the sample set. These 7 samples did not appear to have any particular defining features compared to the other samples, and each had a similar surface area as the other samples. Future studies to determine a correlation between the number of potential sweep cycles and the deposited mass will benefit from the ability to electrodeposit LEU which has a higher specific activity compared to natural uranium, decreasing the counting time required to measure the sample activity

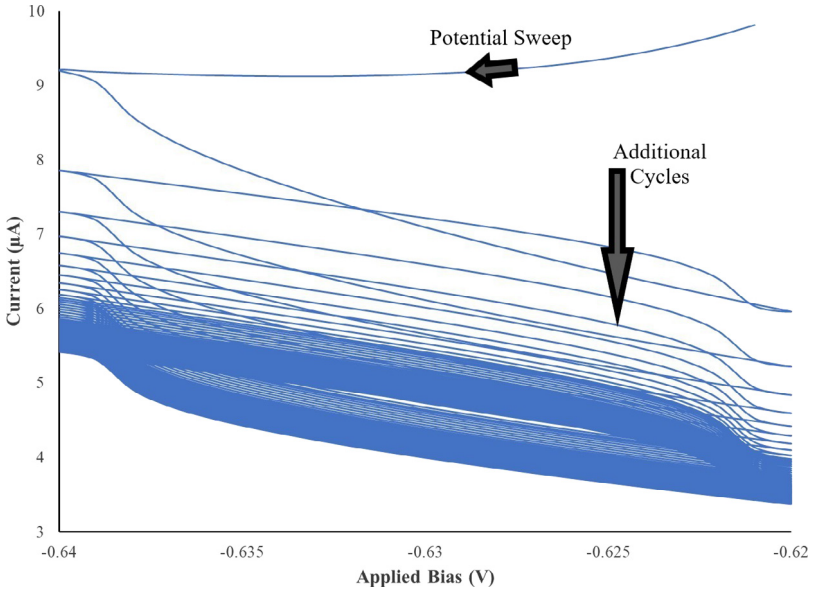

Fig. 6. A characteristic decrease in maximum current was observed on the cyclic voltammogram of sample D.1.48, as well as the other discs.

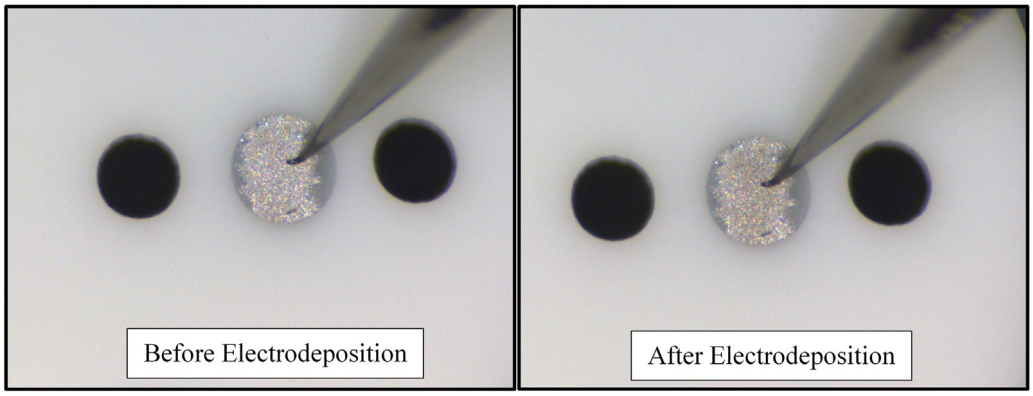

Fig. 7. The metallic electrode turned from silver to gold in colour after electrodeposition.

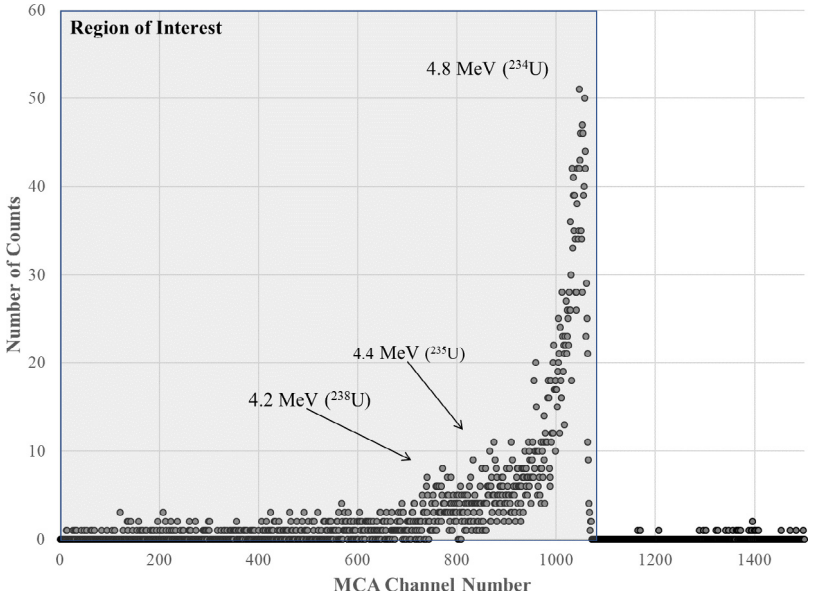

Fig. 8. LEU decays by alpha emission from 3 isotopes (^{234}U, ^{235}U, and ^{238}U), but is dominated by the decay of ^{234}U, identifiable in the alpha-particle pulse-height spectrum which was used to determine the activity of each disc and therefore the mass of uranium electrodeposited, spectrum from sample D.1.48 shown.

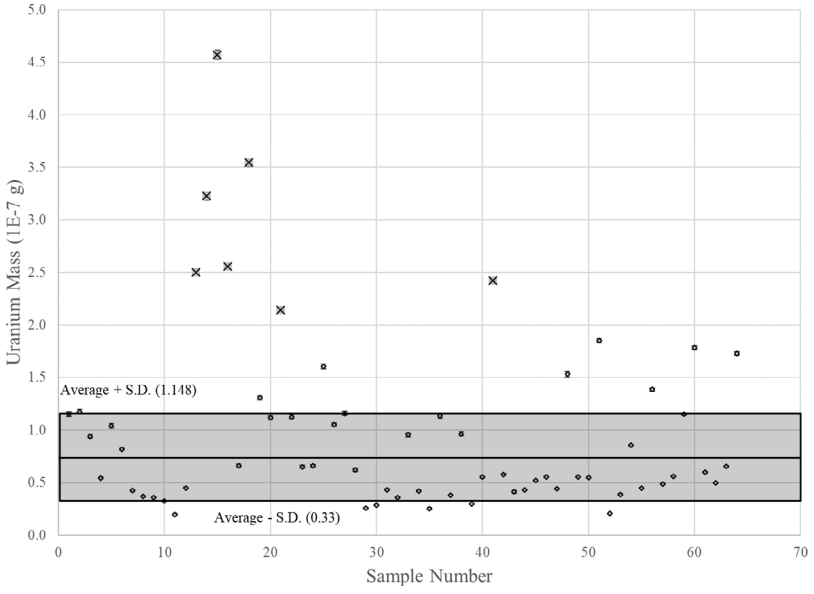

Fig. 9. Disregarding the seven outliers (marked with 'x') improves the standard deviation of electrodeposited samples.

Table 3
The mass of 19.695% enriched uranium deposited on each sample was calculated by measuring the alpha-particle activity, correcting for detector efficiency and background. Error is due to counting statistics alone.

Sample ID	Counts	Time (s)	Measurement efficiency	Background adjusted count rate (cps)	Mass (1×10^{-7} g)	Mass error (1×10^{-9} g)	Error (%)
D.1.1	2636	251487	0.243	0.042	1.15	2.35	2.04%
D.1.2	2690	251579	0.249	0.043	1.18	2.28	1.94%
D.1.3	2124	251655	0.245	0.034	0.94	2.06	2.18%
D.1.4	4269	858292	0.251	0.020	0.54	0.84	1.55%
D.1.5	2422	251690	0.253	0.038	1.04	2.13	2.05%
D.1.6	6495	858355	0.254	0.030	0.82	1.02	1.25%
D.1.7	3330	858387	0.251	0.015	0.42	0.74	1.74%
D.1.8	4173	1224256	0.252	0.013	0.37	0.59	1.61%
D.1.9	4067	1224086	0.253	0.013	0.36	0.57	1.59%
D.1.10	5149	1720178	0.250	0.012	0.33	0.47	1.44%
D.1.11	456	251777	0.248	0.007	0.20	0.94	4.75%
D.1.12	3769	858226	0.250	0.016	0.45	0.87	1.94%
D.1.13	5833	251844	0.255	0.091	2.50	3.27	1.31%
D.1.14	7574	251856	0.256	0.117	3.23	3.71	1.15%
D.1.15	10834	251874	0.259	0.166	4.57	4.39	0.96%
D.1.16	5889	251903	0.252	0.093	2.56	3.33	1.30%
D.1.17	1991	322967	0.243	0.024	0.66	1.61	2.44%
D.1.18	10370	322987	0.249	0.129	3.54	3.49	0.98%
D.1.19	3775	323017	0.245	0.048	1.31	2.14	1.64%
D.1.20	3290	323023	0.251	0.041	1.12	1.95	1.75%
D.1.21	6369	323068	0.253	0.078	2.14	2.69	1.26%
D.1.22	3358	323066	0.254	0.041	1.13	1.95	1.73%
D.1.23	1924	323114	0.251	0.024	0.65	1.49	2.29%
D.1.24	1962	323104	0.252	0.024	0.66	1.50	2.28%
D.1.25	4780	323154	0.253	0.058	1.61	2.33	1.45%
D.1.26	3094	323137	0.250	0.038	1.05	1.90	1.81%
D.1.27	3386	323197	0.248	0.042	1.16	2.00	1.72%
D.1.28	1928	323175	0.250	0.023	0.62	1.54	2.48%
D.1.29	771	323240	0.255	0.009	0.26	0.93	3.62%
D.1.30	5766	2158147	0.256	0.010	0.28	0.39	1.36%
D.1.31	3801	930037	0.259	0.016	0.43	0.71	1.63%
D.1.32	4249	1296065	0.252	0.013	0.36	0.55	1.55%
D.1.33	2375	271677	0.243	0.035	0.95	2.07	2.17%
D.1.34	4762	1244743	0.249	0.015	0.42	0.63	1.50%
D.1.35	623	271737	0.245	0.009	0.25	1.04	4.11%
D.1.36	2816	271762	0.251	0.041	1.14	2.15	1.89%
D.1.37	4404	1245106	0.253	0.014	0.38	0.60	1.58%
D.1.38	2421	271817	0.254	0.035	0.96	1.97	2.04%
D.1.39	4703	1740454	0.251	0.011	0.30	0.44	1.48%
D.1.40	4476	878415	0.252	0.020	0.55	0.84	1.53%
D.1.41	6048	271884	0.253	0.088	2.42	3.11	1.29%
D.1.42	6569	1244778	0.250	0.021	0.58	0.73	1.25%
D.1.43	1017	271931	0.248	0.015	0.41	1.30	3.16%
D.1.44	5275	1244806	0.250	0.016	0.43	0.74	1.72%
D.1.45	9329	1931512	0.255	0.019	0.52	0.54	1.04%
D.1.46	8133	1565321	0.256	0.020	0.56	0.62	1.12%
D.1.47	8059	1931443	0.259	0.016	0.44	0.50	1.12%
D.1.48	3812	272047	0.252	0.056	1.53	2.48	1.62%
D.1.49	11250	2157752	0.243	0.020	0.55	0.68	1.23%
D.1.50	10851	2157846	0.249	0.020	0.55	0.55	1.00%
D.1.51	14310	864266	0.245	0.067	1.85	1.56	0.84%
D.1.52	3269	1726420	0.251	0.007	0.21	0.38	1.83%
D.1.53	3126	864297	0.253	0.014	0.39	0.72	1.85%
D.1.54	17062	2157941	0.254	0.031	0.86	0.66	0.77%
D.1.55	8808	2158000	0.251	0.016	0.45	0.48	1.08%
D.1.56	11001	864324	0.252	0.050	1.39	1.33	0.96%
D.1.57	11310	2525088	0.253	0.018	0.49	0.47	0.96%
D.1.58	10983	2158616	0.250	0.020	0.56	0.55	0.98%
D.1.59	9019	864870	0.248	0.042	1.15	1.22	1.06%
D.1.60	14313	864882	0.250	0.065	1.79	1.57	0.88%
D.1.61	11968	2158675	0.255	0.022	0.60	0.55	0.92%
D.1.62	11757	2524868	0.256	0.018	0.50	0.47	0.94%
D.1.63	13342	2158773	0.259	0.024	0.66	0.57	0.87%
D.1.64	13680	864924	0.252	0.063	1.73	1.48	0.86%

after electrodeposition. Electrodeposition remains an attractive method to deposit small amounts of fissile material onto metallic substrates for the fabrication of MPFDs, and the small electrodes, such as those studied in the present work, will improve the ability of MPFDs to be fabricated in smaller physical geometries.

Acknowledgements

This paper presents work supported by the US Department of Energy Office of Nuclear Energy, USA Contracts DE-NE008408 and DE-AC07-05ID14517. MPFD discs were fabricated and analysed at the Kansas

State University Semiconductor Materials and Radiological Technologies laboratory (Manhattan, KS). Laser Micro-Jet® fabrication was performed at Synova U.S.A (Secaucus, NJ). Sample surface analysis was performed at the Idaho National Laboratory (Idaho Falls, ID).

References

[1] T. Unruh, J. Remp, D. McGregor, P. Ugorowski, M. Reichenberger, NEET Micro-Pocket Fission Detector - FY 2013 Status Report, Idaho national Laboratory, 2013.

[2] T. Unruh, M. Reichenberger, S. Stevenson, K. Tsai, D. McGregor, Enhanced micro-pocket fission detector for high temperature reactors - FY17 final project report, Idaho National Laboratory, Idaho Falls, ID, 2017.

[3] M. Reichenberger, T. George, R. Fronk, P. Ugorowski, J. Geuther, J. Roberts, T. Ito, H. Vo-Le, S. Stevenson, D. Nichols, D. McGregor, Advances in the Development and Testing of Micro-Pocket Fission Detectors (MPFDs), in: IAEA International Conference on Research Reactors: Safe Management and Effective utilization, Vienna, Austria, 2015.

[4] M.A. Reichenberger, Micro-Pocket Fission Detectors: Development of Advanced, Real-Time, in-Core, Neutron -Flux Sensors, Kansas State University, Manhattan, KS, 2017.

[5] C. Jenson, K. Condie, N. Woolstenhulme, T. Unruh, E. Larsen, R. Skifton, P. Calderoni, J. Svoboda, A. Fleming, Z. Hua, H. Ban, M. Reichenberger, J. Roberts, M. Harrison, D. Nichols, W. Fu, K. Kellogg, J. Hewitt, D. McGregor, FY17 report for instrumentation development for the transient testing program, Idaho National Laboratory, Idaho Falls, ID, 2017.

[6] V.K. Patel, M.A. Reichenberger, J.A. Roberts, T.C. Unruh, D.S. McGregor, MCNP6 simulated performance of micro-pocket fission detectors (MPFDs) in the transient reactor test (TREAT) facility, Ann. Nucl. Energy (2017) 191–196.

[7] L.C. Hao, C.V. Tao, N.V. Dong, H.N. Nghi, P.T. Dung, L.V. Thong, Rapid preparation of Uranium and Thorium alpha sources by electroplating technique, Kerntechnik 75 (6) (2010) 381–385.

[8] R.A. Henderson, J.M. Gostic, J.T. Burke, S.E. Fisher, C.Y. Wu, Electrodeposition of U and Pu on thin C and Ti substrates, Nucl. Instrum. Methods A 655 (2011) 66–71.

[9] O.A. Dumitru, R.C. Begy, D.C. Nita, L.D. Bobos, C. Cosma, Uranium electrodeposition for alpha spectrometric source preperation, J. Radioanal. Nucl. Chem. 298 (2013) 1335–1339.

[10] C. Ingelbrect, A. Moens, R. Eykens, A. Dean, Improved electrodeposited actinide layers, Nucl. Instrum. Methods A 397 (1) (1997) 34–38.

[11] M.A. Reichenberger, T. Ito, P.B. ugorowski, B.W. Montag, S.R. Stevenson, D.M. Nichols, D.S. McGregor, Electrodeposition of uranium and thorium onto small platinum electrodes, Nucl. Instrum. Methods A (812) (2016) 12–16.

[12] U.S.A. Synova, The Laser MicroJet Technology, Synova USA, 2018 [Online]. Available: https://www.synova.ch/technology/laser-microjet.html. (Accessed 25 April 2018).

[13] U.S. Goverment Publishing Office, 49CFR173434, 1 10 1998 [Online]. Available: https://www.gpo.gov/fdsys/pkg/CFR-2010-title49-vol2/pdf/CFR-2010-title49-vol2-sec173-434pdf. (Accessed 24 April 2018).